(Preprint) AAS 20-021

PASSIVE ROLL STABILIZATION OF THE NEAR EARTH ASTEROID SCOUT SOLAR SAIL MISSION

Ivan Rodrigues Bertaska,[*] Andrew Heaton,[†] Juan Orphee,[‡] and Benjamin Diedrich[§]

The Near Earth Asteroid (NEA) Scout is a small satellite, solar sail mission set to launch on Artemis I. Analysis of the NEA Scout solar radiation pressure model determined that, for certain solar incidence angles, there exists at least one locally stable equilibrium point about the "roll" axis, or the axis normal to the solar sail plane. This analysis is extended to three other geometrically similar solar sail models, and a Lyapunov stability analysis is conducted demonstrating that the stable equilibria are locally stable for the majority of roll angles in a wide range of solar incidence angles. Under certain assumptions, it is possible that only two axis control is required for non-spinning solar sails. If the roll axis is controlled, an active rate damping controller can be designed to asymptotically stabilize the system. Simulation results are presented that follow the stability analysis, where in the homogenous case, the system enters a limit cycle and, in the actively damped case, the system asymptotically converges to the equilibrium point.

INTRODUCTION

The Near Earth Asteroid (NEA) Scout is a 6U CubeSat propelled by a deployable 84.9m^2 solar sail.[1,2] Solar sail propulsion provides an attractive alternative to traditional chemical propulsion systems. Propellant does not need to be loaded onboard spacecraft, and the propulsion system does not need be powered, heated, or conditioned. This provides a volume and mass savings that can be allocated towards more payload. However, solar sails create challenges to the Attitude Determination and Control System (ADCS) designer. The large surface of the sail creates solar radiation pressure (SRP) torques that are several orders of magnitude larger than traditional propulsion designs. Additionally, solar sail propulsion provides the most benefit in reaching far targets in deep space, where magnetic torque rods cannot be used for momentum management. For both solar sail and chemical systems, this typically requires the ADCS to desaturate the spacecraft momentum using a chemical reaction control system (RCS).

This work examines the effect of the solar radiation pressure on the stability of the "roll" axis of the sail, i.e., the rotational axis normal to the sail plane. In Figure 1, the "roll" axis corresponds with the z-axis of NEA Scout. For certain solar incidence angles (SIA), a stable equilibrium point exists where SRP torques will cause the spacecraft to converge to an equilibrium where the magnitude of the roll SRP torque is at a minimum. This effect is entirely passive and requires no active

[*]NEA Scout ADCS, EV41 Control Systems Design & Analysis, NASA MSFC, Huntsville, AL, 35812
[†]NEA Scout ADCS Lead, EV42 Mission Analysis Guidance & Navigation, NASA MSFC, Huntsville, AL, 35812
[‡]NEA Scout ADCS, EV42 Mission Analysis Guidance & Navigation, NASA MSFC, Huntsville, AL, 35812
[§]NEA Scout ADCS, EV42 Mission Analysis Guidance & Navigation, Dynamic Concepts Inc., Huntsville, AL, 35812

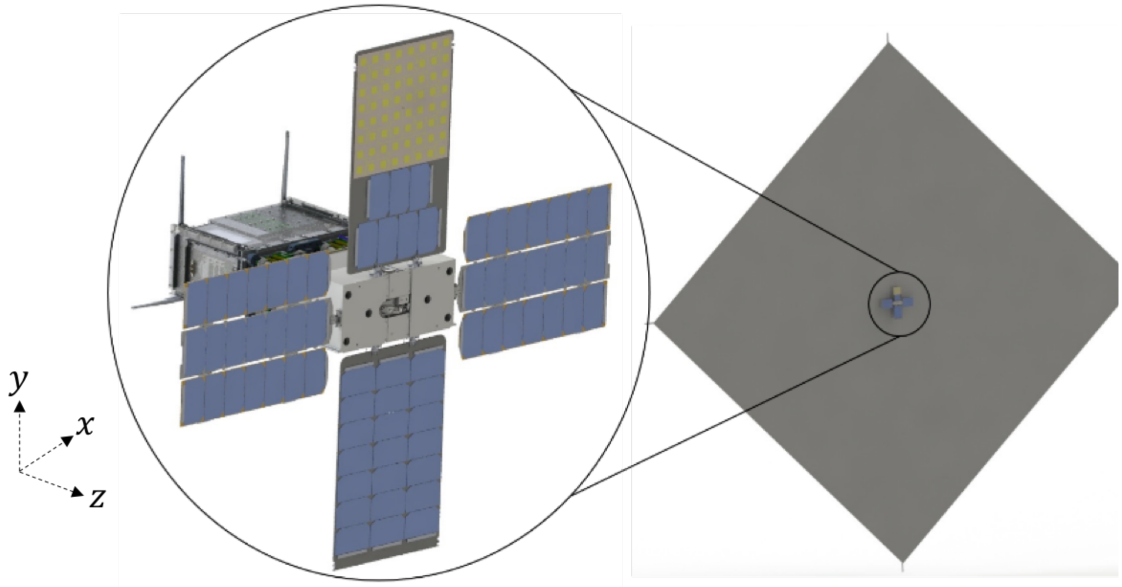

Figure 1. The NEA Scout spacecraft before sail deployment (left) and after sail deployment (right). The solar sail is deployed from the middle of the spacecraft bus and covers an area of 84.9m^2.

stabilization – the only requirement is that the spacecraft center of mass is not coincident with the sail center of pressure. It should be noted that, for the NEA Scout sail geometry, the roll axis does not affect the thrust vector of the sail and produces no impacts to the trajectory. If there are no other constraints on the roll angle (e.g., science objectives, ground communications, etc.), the ADCS designer can choose one that reduces momentum accumulation, and as a result, conserves propellant.

Allowing an axis to be passively controlled produces a number of benefits. A large increase in propellant savings can be achieved by reducing the number of axes for momentum management. Additionally, solar sail missions may only require two axis stabilization for certain mission concepts. The former will be employed during the NEA Scout mission, where the small size of the 6U platform limits the amount of propellant margin. A sail characterization as in Reference 3 will be used to estimate the sail torques. Although the trajectory design will dictate the clocking and incidence of the sail thrust vector along the sun-line, the roll about the thrust vector will be chosen such that it minimizes the number of momentum management events about that axis.

Additionally, the NEA Scout spacecraft is equipped with an Active Mass Translator (AMT) where roughly 40% of its mass can be translated along the sail plane. This allows for the center of mass (CM) to be translated to a point where the SRP torques are minimized. This device is also used for momentum management about the spacecraft's "pitch" and "yaw" axes, where the CM is adjusted such that the SRP torques oppose the built-up momentum in those axes. Outfitting a spacecraft with such a system (or with alternatives that change the center of pressure, such as reflectivity control devices)[4], opens the possibility of a completely propellant-less spacecraft for deep space applications, as the "roll" axis can be passively stabilized through structural damping or nutation dampers.

The structure of this paper is as follows: the first section provides background on solar sails and recent advances in solar sailing technology, as well as a brief mission overview for NEA Scout. The subsequent section defines the rigid body dynamics of a deep-space solar sail mission. In the ensuing section, three simple solar sail geometric configurations are presented, and a Lyapunov stability analysis is conducted for the homogenous case with a generalized function representing the solar radiation pressure torques. In the next section, simulation results are presented for an actively damped system. This paper closes with some concluding remarks and suggestions for forward work.

BACKGROUND

Solar sails operate off the momentum exchange between photons and the reflective sail. While a photon is massless, it does have a very small amount of momentum proportional to its frequency. The combined solar flux on the sail produces a pressure distribution across the sail. When integrated, the total thrust and center of pressure can be calculated. The offset between the center of pressure and the center of mass creates a constant torque the ADCS must overcome. Momentum management of solar sail spacecraft is still an open problem, but solutions, such as the AMT on NEA Scout or reflectivity changing devices, have been proposed to reduce the separation between the center of mass and the center of pressure.

Although the concept of solar sail propulsion dates back nearly 100 years to Soviet-era scientists Konstantin Tsiolkovsky and Fridrickh Tsander, solar sails have only recently been employed as the main propulsion system on spacecraft.[5] The IKAROS mission from JAXA was the first successful use of a solar sail as the main propulsion system of a spacecraft.[6] The same year, NASA launched the NanoSail-D2 mission onboard the FASTSAT spacecraft. This was the first on-orbit demonstration of a solar sail deployment by the American space agency. Although NanoSail-D2 was not actively stabilized, ground observations of the spacecraft allowed engineers at Marshall Space Flight Center to reconstruct its attitude and estimate the center of pressure of the sail.[7]

Future sail mission concepts continue to further the technology. Solar Cruiser is a proposed NASA mission that was recently funded for a nine-month concept study. Solar Cruiser would feature an order of magnitude increase in sail size to 1600m^2. A heliophysics mission, Solar Cruiser will travel below the Sun-Earth L1 Lagrange point and hold a stationary orbit above the solar system ecliptic plane. Additionally, the National Oceanic and Atmospheric Administration have examined solar sail spacecraft as part of their space weather prediction system due to their ability to station-keep at distances closer to the sun than the L1 Lagrange point.[8]

Near Earth Asteroid Scout Mission and Overview

The NEA Scout spacecraft is an interplanetary solar sail mission in the form of a 6U CubeSat. Its main science objective is to image a near earth asteroid, providing valuable information on the asteroid's ephemeris, rotation rate, albedo, and morphology. It is one of the thirteen secondary payloads on the Artemis I mission – the maiden launch of the Space Launch System (SLS) with Orion Crew Module (CM). All secondary payloads are housed on the Orion Stage Adapter (OSA), which interfaces the Orion CM to the SLS upper stage, the Interim Cryogenic Propulsion Stage (ICPS). Once the Orion CM separates from ICPS, the secondary payloads will be released at five different "bus stops." Once released, NEA Scout will perform a trajectory correction maneuver (TCM) using an R-236fa cold gas propulsion system, and then deploy an 84.9m^2 solar sail. It should be noted that the thrust from the solar sail is not sufficient to meet the time constraints of the TCM, and the spacecraft must rely on a traditional chemical propulsion system. However, the chemical propulsion system alone would not be sufficient to reach the target asteroid – the solar sail will produce the majority of the ΔV for the mission. Figure 1 shows NEA Scout before sail deployment (left) and after sail deployment (right).

NEA Scout is a three-axis stabilized spacecraft. For attitude determination, a modified Blue Canyon Technology NST Star Tracker and a Sensonor STIM300 inertial measurement unit (IMU) are sampled at 5Hz and 10Hz, respectively. An extended Kalman filter fuses these measurements to obtain an estimate of the spacecraft state. Four Blue Canyon Technology 15mN-m-s reaction wheels are included in a tetrahedral configuration for fine pointing during transit and science pointing. A VACCO R-236fa cold gas reaction control system (RCS) is used for detumbling the spacecraft, performing the trajectory correction maneuver, and momentum management. It features two axial thrusters, used during the TCM, and four off-axial thrusters for coarse control of the spacecraft attitude and to desaturate the reaction wheels.[2]

Active Mass Translator and Momentum Management

Although the RCS has the capability to manage the spacecraft momentum in all three axes, the primary method to desaturate the reaction wheels is through the active mass translator. The AMT is capable of moving 4.3kg (out of a total of 10.8kg) of the spacecraft mass along the sail plane. The translation range is limited by the bus dimensions and cable routing to be from -80mm to 30mm in the spacecraft x-axis, and +/-34mm in the y-axis. This device allows for the center of mass to be translated, reducing the offset from the center of pressure, and thus, minimizing the solar radiation pressure torques. A Proportional-Integral (PI) controller examines the built-up spacecraft momentum along all three axes and positions the AMT such that the momentum is minimized. This effectively performs propellant-less momentum management about the pitch and yaw axes and minimizes the SRP disturbance torque about the roll axis.

SPACECRAFT DYNAMICS

This section provides a brief overview of the clocking, solar incidence angle, and roll angle used to define the orientation of the sail normal with respect to the sun-line. It also details the rigid body equations of motion for the spacecraft bus, neglecting parasitic flexible body dynamics from the sail.

Clocking, Solar Incidence Angle, and Roll

For solar sail missions, it is of primary importance to relate the spacecraft attitude (and thrust vector) to the sun-line. Figure 2 depicts the two angles used to express this relationship. The sun-line, $\hat{r} \in \mathbb{R}^3$ is defined as the vector from the centroid of the sun to the spacecraft frame origin. The solar incidence angle, $\alpha \in \mathbb{S}$, also called the solar cone angle or angle of incidence, is the angle formed between the sail normal, $z \in \mathbb{R}$, and the sun-line, i.e., the dot product of the sail normal and the sun-line will produce the cosine of the solar incidence angle. The clocking angle, $\delta \in \mathbb{S}$ is the extrinsic rotation of sail normal about the sun-line. Expressed in other terms, the clocking angle is the rotation from the projection of the sail normal to a plane normal to the sun-line. The final component used to define the rotation from the sun frame to the body frame is roll, $\psi \in \mathbb{S}$. This is the rotation about the sail normal, i.e., about the thrust vector. Taken together, the clock, SIA, and roll angles comprise a 3-2-3 Euler angle rotation from an arbitrary solar frame to the body frame.

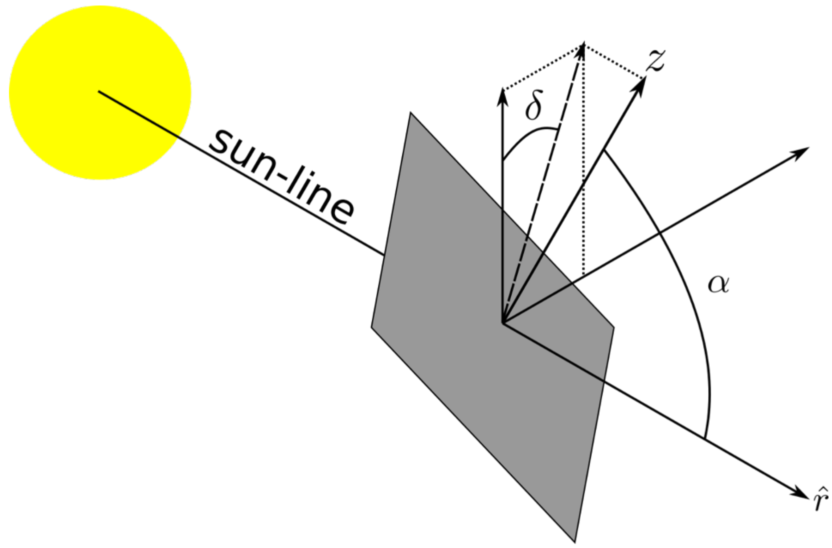

Figure 2. Clocking angle δ and solar incidence angle δ with respect to the sun-line $\hat{r}$.

RIGID BODY SPACECRAFT DYNAMICS

Neglecting parasitic flexible body dynamics from the sail and momentum contribution from the reaction wheels, the 3DOF equations of motion for a solar sail can be expressed as,

$$I\dot{\omega} + \omega^{\times} I\omega = \tau_{ctrl} + \tau_{dist}, \tag{1}$$

where $I \in \mathbb{R}^{3\times3}$ is the mass moment of inertia of the spacecraft, $\omega \in \mathbb{R}^3$ are the three body rates, $\tau_{ctrl} \in \mathbb{R}^3$ are the control torques from the ADCS, and τ_{dist} are the disturbance torques. For a mission like NEA Scout, where the majority of the mission will be in deep space away from large bodies, the disturbance torques will be dominated by the SRP, $\tau_{dist} \approx \tau_{SRP}(\alpha, \delta, \psi)$.

For a non-spinning sail, the roll axis equation can be decoupled from the pitch and yaw terms, and becomes purely a function of the control torque and the SRP torque,

$$I_{zz}\ddot{\psi} = \tau_{ctrl,z} + \tau_{SRP,z}(\alpha, \delta, \psi). \tag{2}$$

LYAPUNOV STABILITY ANALYSIS OF SOLAR SAIL ROLL AXIS

Once the equations of motion for the roll axis have been defined, it is straightforward to determine the stability of the system in the presence of only solar radiation pressure torques. Although this process is dependent on the calculation of the solar radiation pressure torques on the sail, that derivation is left out of this work for brevity. The SRP torque calculation used in this section follows that of Reference 9.

Motivating Examples: Symmetric, Asymmetric and Asymmetric "Concave" Sails

Three different sail models are presented in this section in order of increasing complexity. All are similar in footprint, and thus, exhibit similar thrust. The "symmetric flat" sail is the traditional flat-plate sail approximation where the two halves of the sail are identical. The "asymmetric sail" shortens one half, creating an asymmetry. Similarly, the "asymmetric concave" sail model displays an asymmetry about the flat-plate sail plane, but also has an asymmetry in the direction of the sail normal. The term "concave" refers to the deformation of the sail normal to its undeformed axis,

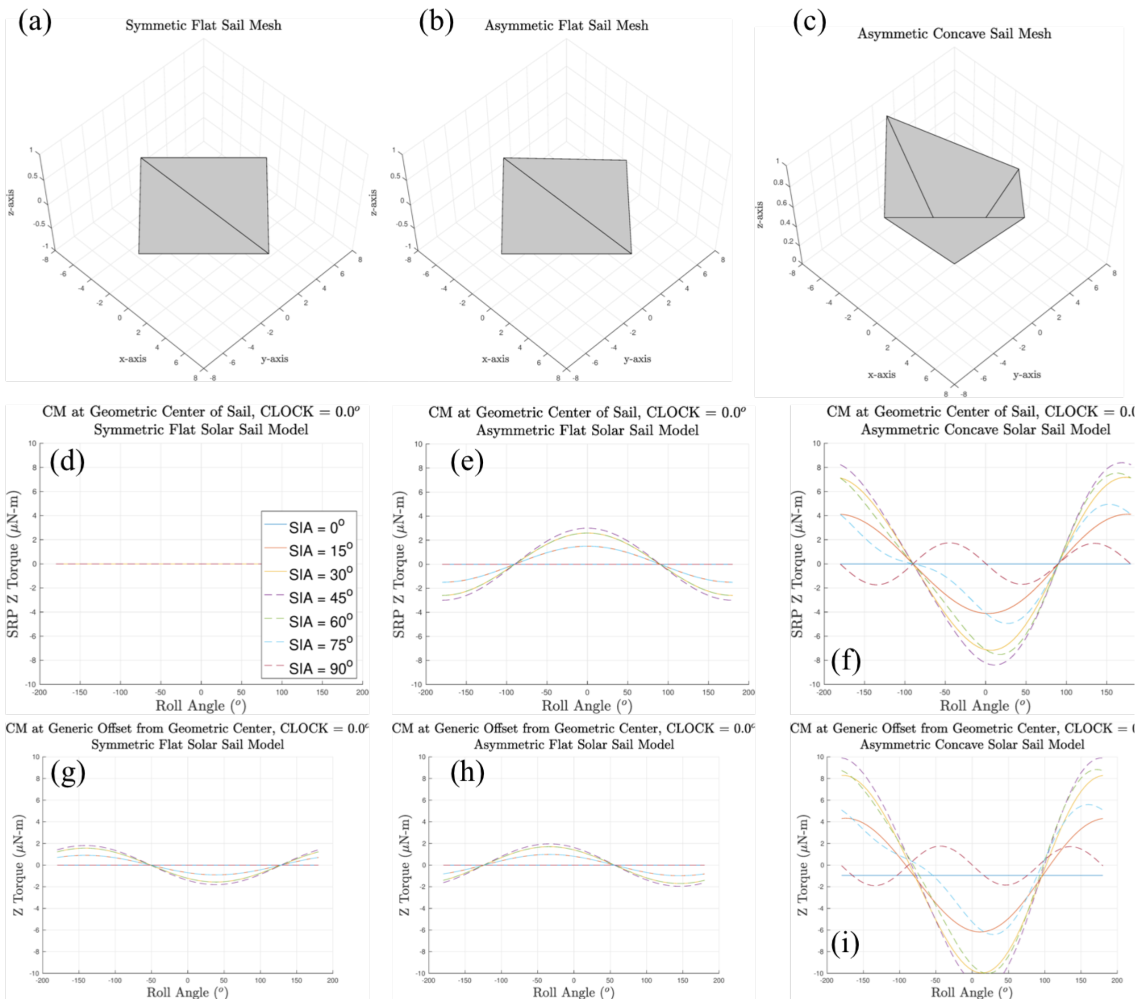

Figure 3. Different sail geometries with the CM at the geometric center of the ideal, symmetric, flat sail (middle row) and with the CM offset from this location (bottom row) for different solar incidence angles (SIA).

forming a concavity with respect to the sun. The SRP torques about the roll axis were calculated for different solar incidence angles, and the results are displayed in Figure 3. These torques were calculated assuming the CM was centered in one of two locations. The middle row assumes that the CM is located at the geometric center of the *ideal sail* for all three sail models. The bottom row shifts the CM 40mm in the x-axis and 50mm in the y-axis (the maximum allowable CM offset from the Planetary Systems Corporation 6U CubeSat dispenser).

The first key takeaway is that SRP roll torque about the symmetric sail with the CM at the geometric center of the sail (Figure 3d) does not vary with solar incidence angle nor roll. This is because the CM and the sail center of pressure remain fixed at the same location regardless of SIA. Once the CM is offset, or there is an asymmetry in the sail (Figure 3g, Figure 3e, or Figure 3h), the SRP torque varies about the roll axis in a sinusoidal profile. This oscillatory response becomes more pronounced when the sail is deformed normal to the ideal sail plane (Figure 3f and Figure 3i). However, an important thing to note is that all of these torque profiles exhibit at least two zero crossings for these SIAs.

In the asymmetric concave case, it is apparent that there is a small bias across all roll angles. For SIAs close to 0º, the zero-crossing may not exist. However, typical deep-space mission designs aim to maximize the amount of thrust in a component tangent to the spacecraft's orbit. For a near ideal sail, this will lead to a desired SIA around 45 degrees for the majority of the mission. This also coincides with the maximum SRP torque curves in Figure 3, making it likely that there will be at least two zero-crossings.

For a deep space mission, where all other environmental disturbances are dominated by the SRP torques, these torque profiles effectively represent the phase-plane of the spacecraft in the homogenous case. It is apparent then that the zero-crossings are equilibrium points. Following Lyapunov's first method for determining stability, those equilibrium points with positive derivatives are unstable equilibria, while those exhibiting negative derivatives are stable (in the sense of Lyapunov). The subsequent section presents a more rigorous stability analysis demonstrating that this system is locally stable, but not necessarily asymptotically stable, within a neighborhood of the stable equilibria.

Although these sail shapes are geometrically simple, they are a close representation of the SRP roll torques for NEA Scout (Figure 4). The SRP roll torque profile of NEA Scout most closely resembles that of Figure 3i. Furthermore, deployment of the thin, gossamer sail material is, presently, a process with many uncertainties. It is highly unlikely that the deployment event will yield a nearly perfectly symmetric sail, where the solar radiation pressure torque response is not sufficient to stabilize the roll axis. In addition, during the mission, the sail will be subject to a substantial amount of heat, further deforming its shape into a more "concave" geometry.

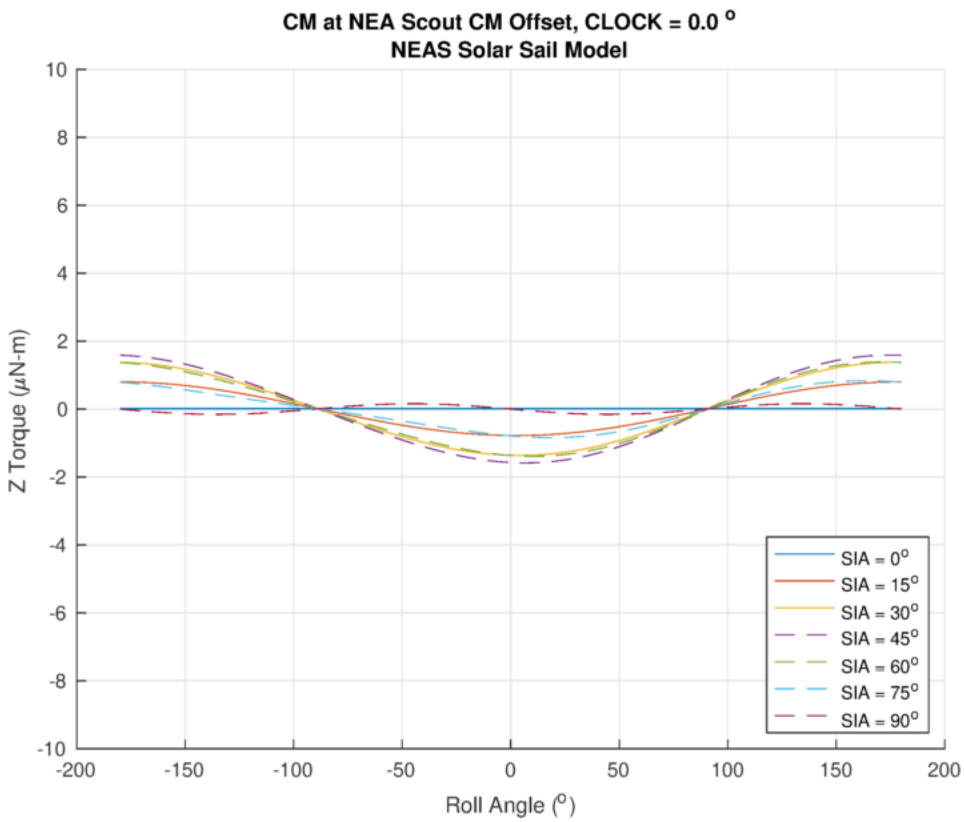

Figure 4. NEA Scout sail model SRP roll torque with respect to different clocks and solar incidence angles. This model takes into account thermal deformations of the sail and presents a best estimate of the sail shape through the majority of the mission.

Lyapunov Stability Analysis of Solar Radiation Pressure Torques

This section presents the Lyapunov stability analysis of the roll dynamics in Eq. (2). In the homogenous case, where $\tau_{ctrl,z} = 0$, the roll angular acceleration is a solely dependent on the SRP roll torque, which is a function of the clocking angle, SIA, and roll angle. Since the roll dynamics will not influence the clocking angle or the SIA, the roll axis will be subject to a single sinusoidal-like torque profile, as in Figure 3 or Figure 4. For large enough SIAs, there exists at least one locally stable equilibrium point. A neighborhood around this point can be defined that will guarantee stability (in the sense of Lyapunov). This is a classical nonlinear dynamics problem, and the succeeding analysis generally follows that in Reference 10.

Substituting $x \in \mathbb{R}$ for $\psi - \psi_e$ (where ψ_e is the locally stable equilibrium point) and defining $g(x) : \mathbb{R} \to \mathbb{R}$ to be the *opposite* of the SRP torque profile such that $g(0) = 0$, Eq. (2) fits the form of,

$$\ddot{x} = -g(x). \tag{3}$$

By inspection, $g(x)$ is locally Lipschitz, and a domain $D = (a, b)$ about $x = 0$ can be defined such that,

$$xg(x) > 0 \; \forall x \neq 0 \; and \; x \in (a, b). \tag{4}$$

A positive definite Lyapunov function $V(x) : \mathbb{R} \to \mathbb{R} \geq 0$ is defined such that $V(x) > 0 \; \forall x \in D - \{0\}$,

$$V(x) = \int_0^x g(y)\, dy + \frac{1}{2}\dot{x}^2. \tag{5}$$

To determine the stability of the system using Lyapunov's second method, the derivative of the Lyapunov function $V(x)$ must be ensured to be negative semidefinite,

$$\dot{V}(x) = g(x)\dot{x} - g(x)\dot{x} = 0 \; \forall x \in D. \tag{6}$$

Thus, Eq. (2) is locally stable (in the sense of Lyapunov) in a neighborhood D about the stable equilibrium point. As long as a locally stable zero-crossing exists in the torque profile for the desired SIA, these neighborhoods can be defined for all roll angles with the exception of the unstable equilibrium points. An undamped pendulum is a good mechanical analogy for this system, where a stable and unstable equilibrium point exists. Any perturbation off of the unstable equilibrium will yield a limit cycle oscillation about the stable equilibrium point.

An important distinction is that the system is not proven to be *asymptotically* stable. Eq. (2) does not include any energy damping mechanism. For a non-zero initial condition, the system will oscillate about the equilibrium point in a limit cycle oscillation. Although this effect is guaranteed to be stable, it is not desirable to the control designer. However, it is feasible to prove local asymptotic stability by taking into account possible sources of damping, like internal friction, or to include passive dampers, like nutation dampers, in the spacecraft design. Solar sails are thin, gossamer materials subject to flexible body dynamics. It is possible that the structural damping in the sail is sufficient to stabilize the system, although accurately characterizing this value on the ground, under the effects of gravity, is still an open problem.

Figure 5 depicts a simple representation of a stable equilibrium point for a mass-less, asymmetric sail at an arbitrary solar incidence angle to the sun. Due to the asymmetry in the sail halves, the right half of the experiences a greater SRP force, as well as a larger CM-CP offset. This is sufficient to provide a restoring moment for any perturbations off the equilibrium point.

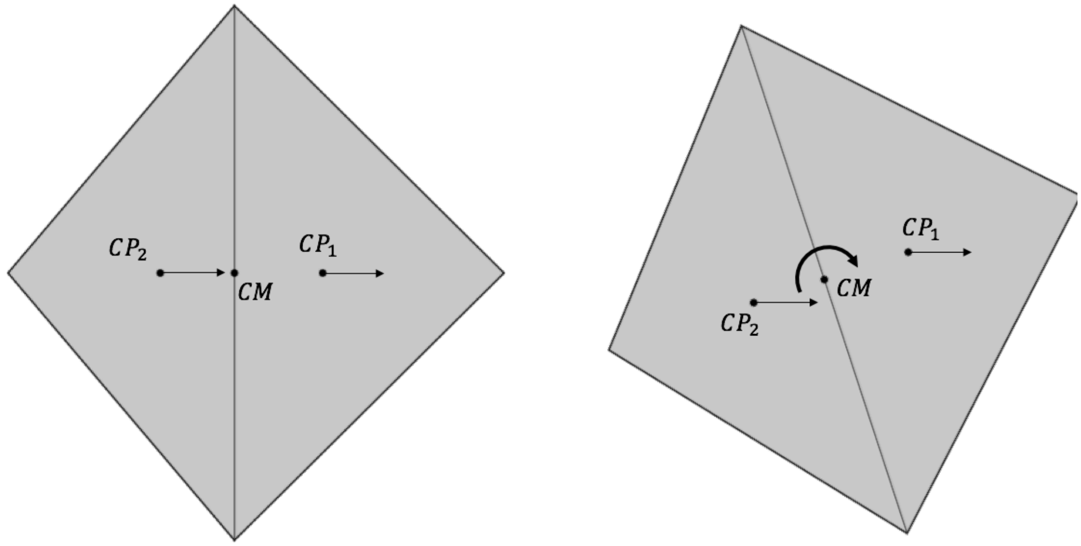

Figure 5. An asymmetric sail at a stable equilibrium point. The left half the sail has a smaller area than the right half, and as a consequence, has a smaller separation between the CM and the CP. When the spacecraft is perturbed about the roll angle, there is a restoring force that brings it back to the equilibrium point (right).

NEA SCOUT ROLL STABILIZATION SIMULATIONS

Although the roll axis will be passively stable for certain non-spinning solar sail configurations at a range of solar incidence angles, damping can be provided if the spacecraft is capable of effecting in that axis. As NEA Scout requires three-axis stabilization to meet science objectives, a rate damping controller can be constructed that adds damping to the closed loop system. Examining Eq. (2) and performing the $x = \psi - \psi_e$ substitution as in Eq. (3), the rate damping controller is defined as $\tau_{ctrl,z} = -k_d \dot{x}$, leading to the following equation,

$$Izz\ddot{x} = -k_d \dot{x} - g(x). \tag{7}$$

A Taylor series expansion is performed on $g(x)$. Keeping only the first order terms yields a linear system,

$$Izz\ddot{x} \approx -k_d \dot{x} - \frac{\partial g}{\partial x}_{x=0} x = -k_d \dot{x} - Ax. \tag{8}$$

This equation is a good approximation for the system around the stable equilibrium point $x = 0$. Taking a Laplace transform for the initial conditions $x(0) = x_0$ and $\dot{x}(0) \approx 0$, produces the second-order transfer function for $X(s)$.

$$X(s) = \frac{1}{I_{zz}} \frac{1}{s^2 + k_d/I_{zz}\, s + A/I_{zz}} = \frac{\omega_n^2}{s^2 + 2\zeta\omega_n s + \omega_n^2}. \tag{9}$$

The derivative gain, $k_d \in \mathbb{R} > 0$, can be chosen according to the desired closed loop damping of the system.

A model of Eq. (7) was implemented in Mathworks Simulink and simulated for 15,000s. Initial conditions were setup such that the initial roll angle was a small perturbation off of the unstable equilibrium point. The SRP roll torques were defined according to the symmetric sail model with CM offset from the geometric center of the sail (Figure 3g) at a solar incidence angle of 45°. For these simulations, the stable equilibrium point was defined at $\psi = 0$, and thus, $x = \psi$.

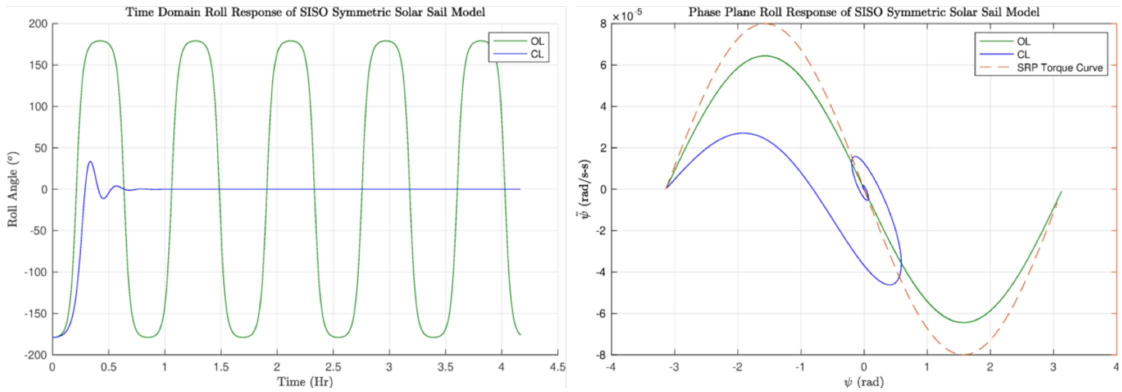

Figure 6. Time domain response (left) and phase plane trajectory (right) of the open loop (green) and rate damped solar sail models (blue). Both simulations were initiated from the unstable equilibrium point, but only the actively damped system is shown to be locally asymptotically stable.

Figure 6 displays the results for the homogenous case of $\tau_{ctrl.z} = 0$ and the actively damped case $\tau_{ctrl,z} = -k_d\dot{\psi}$ in the time domain (left) and the trajectory in the phase plane (right). No passive damping was modeled in the system. The uncontrolled case entered a limit cycle oscillation, as predicted by the stability analysis in the previous section. However, with the addition of an active rate damping controller, damping was added to the closed loop system, and the roll angle was brought to the stable equilibrium point at $\psi = 0$ in 30 minutes.

Although the ADCS system for NEA Scout has this active damping capability, it is not baselined to be used in the nominal case. There is sufficient propellant margin to control all three axes of the spacecraft throughout its two-and-a-half-year mission. However, the roll torque profile will be characterized, and nominal roll angle will be commanded such that the momentum accumulation in the roll axis will be minimized.

CONCLUSION

In summary, a stability analysis of the effect of solar radiation pressure on the "roll" axis of a solar sail spacecraft in the absence of other external disturbances was presented. This analysis is valid for non-spinning, deep space solar sail missions, like NEA Scout. For the ideal-flat plate sail model, as long as the center of pressure of the sail is not coincident with the center of mass, there will exist a stable equilibrium point and an unstable equilibrium point for solar incidence angles greater than 0º and less than 90º. For other sail geometries, these equilibria may exist depending on solar incidence angle. A Lyapunov stability analysis demonstrated for these systems that, effectively, all roll angles with the exception of the unstable equilibria lead to a limit cycle about the stable equilibrium point. With the additional modeling of structural damping or the use of nutation dampers, the stable equilibria will be asymptotically stable. Depending on the mission concept, the roll axis of the solar sail may not need to be actively controlled. If a spacecraft does have active control about the roll axis, a rate damping controller can be designed such that the stable equilibria become asymptotically stable. Simulation results were presented that demonstrated this effect.

Potential avenues to continue this work includes characterization of the solar radiation torque profile in orbit and validation of the NEA Scout solar sail mesh model in Figure 4. Additionally, a structural damping model can be refined to determine the settling time of a passively damped roll axis.

REFERENCES

[1]J. Orphee, B. Diedrich, B. Stiltner, C. Becker and A. Heaton, “Solar Sail Attitude Control System for the NASA Near Earth Asteroid Scout Mission,” *4th Internal Solar Sail Symposium*, 2017.

[2]B. Stiltner, B. Diedrich, J. Orphee, A. Heaton, C. Becker, and I. R. Bertaska “Cold Gas Reaction Control System for the Near Earth Asteroid Scout CubeSat,” *AIAA Space and Astronautics Forum and Exposition*, p. 5185, 2017.

[3]L. Rios-Reyes, “Solar sails: modeling, estimation, and trajectory control,” *University of Michigan*, 2006.

[4]D. Tyler, A. Heaton, J. Munday, and T. Lockett, “Reflectivity Control Device Attitude Control for Solar Cruiser and Future Solar Sail Missions,” *AAS Rocky Mountain Guidance, Navigation, and Control Conference*, 2019.

[5]C. R. McInnes, “Solar sailing: technology, dynamics, and mission applications.” *Springer Science & Business Media*, 2004.

[6]O. Mori, H. Sawada, R. Funase, M. Morimoto, T. Endo, T. Yamamoto, Y. Tsuda, Y. Kawakatsu, J. Kawaguchi, Y. Miyazaki, Y. Shirasawa, and IKAROS Demonstration Team and Solar Sail Working Group, “First Solar Power Sail Demonstration by IKAROS,” *Transactions of the Japan Society for Aeronautical and Space Sciences, Aerospace Technology Japan*, p. 425-431, 2010.

[7]A. Heaton, B. Faller, and C. Katan, “NanoSail – D Orbital and Attitude Dynamics,” *Advances in Solar Sailing*, Springer, Berlin, Heidelberg, p. 95-113, 2014.

[8]M. Lazzara, A. Coletti, and B. Diedrich, “The possibilities of polar meteorology, environmental remote sensing, communications and space weather applications from Artificial Lagrange Orbit,” *Advances in Space Research*, Vol 48, no. 11, p.1880-1889, 2011.

[9]L. Rios-Reyes and D. J. Scheeres, “Generalized model for solar sails,” *Journal of Spacecraft and Rockets*, Vol 42, no. 1, p. 182-185, 2005.

[10]H. K. Khalil, “Nonlinear systems,” *Uppser Saddle River*, 2002.